Free Radical Research, February 2006; 40(2): 147–153

Nitrotyrosine formation and apoptosis in rat models of ocular injury

MUTAY ASLAN[1], İCLAL YÜCEL[2], YUSUF AKAR[2], GÜLTEKIN YÜCEL[1], M. AKIF ÇIFTÇIOĞLU[3], & SALIH SANLIOGLU[4]

Department of Biochemistry, Akdeniz University Medical School, Antalya 07070, Turkey, Department of Ophthalmology, Akdeniz University Medical School, Antalya 07070, Turkey, Department of Pathology, Akdeniz University Medical School, Antalya 07070, Turkey, and Department of Human Gene Therapy Unit, Akdeniz University Medical School, Antalya 07070, Turkey

Accepted by Dr T. Grune

(Received 25 July 2005; in revised form 30 September 2005)

Abstract

This study was performed to examine inducible nitric oxide synthase (NOS-2) expression, nitrotyrosine formation and apoptosis in rats with elevated intraocular pressure (IOP) and/or ocular inflammation. Ocular inflammation was induced via injection of intra-vitreal lipopolysaccharide (LPS) while IOP was elevated by episcleral vessel cauterization. Animals were randomized to one of the following conditions: elevated IOP, LPS, elevated IOP + LPS, and control. Immunohistochemical staining and western blot analysis of retinal lysates revealed NOS-2 and nitrotyrosine immunoreactivity in all disease groups. NOS-2 expression and protein nitration was significantly greater in rats with elevated IOP + LPS compared to elevated IOP, LPS, and control groups. Nitrite levels in the retina affirmed significantly increased levels of nitric oxide generation in LPS-treated rats with elevated IOP ($346 \pm 23.8\,\mu M$) *vs* LPS-treated, elevated IOP and control groups (195.6 ± 12.6, 130 ± 2.5 and $76.6 \pm 15.6\,\mu M$, respectively). Retinal TUNEL staining showed apoptosis in all diseased groups. Percent of apoptotic cells was significantly greater in the elevated IOP + LPS group compared to LPS-treated or elevated IOP groups. Presented data illustrates that both elevated IOP and ocular inflammation augment NOS-2 expression, retinal protein nitration and apoptosis in rats.

Keywords: *Nitrotyrosine, inducible nitric oxide synthase, apoptosis, intraocular pressure, lipopolysaccharide*

Abbreviations: *GCL, ganglion cell layer; INL, inner nuclear layer; IOP, intraocular pressure; IPL, inner plexiform layer; LPS, lipopolysaccharide; NO, nitric oxide; NO_2^-, nitrite; NO_2Tyr, nitrotyrosine; NO_3^-, nitrate; NOS-2, inducible nitric oxide synthase; ONL, outer nuclear layer; OPL, outer plexiform layer; PBS, phosphate buffered saline; PMN, polymorphonuclear; VCL, photoreceptor cell layer*

Introduction

Glaucoma is a degenerative eye disease and is the leading cause of blindness in the United States and other industrialized countries [1]. Experimental studies of induced pressure elevation in nonhuman primates results in typical glaucomatous optic nerve damage [2,3]. Intraocular inflammation, most often termed as uveitis, is also a major cause of severe visual impairment [4]. Recent studies have highlighted the role of nitric oxide (NO) in uveitis and glaucoma by reporting the presence of NOS-2 in the iris-ciliary body [5], retina [6] and in the glaucomatous optic nerve head of experimental rat models [7].

Nitric oxide is an important mediator of homeostatic processes in the eye, such as regulation of aqueous humor dynamics, retinal neurotransmission

Correspondence: M. Aslan, Department of Biochemistry, Akdeniz University Medical School, 07070 Antalya, Turkey. Tel: 90 242 2274343 44126. Fax: 90 242 2274482. E-mail: mutayaslan@akdeniz.edu.tr

ISSN 1071-5762 print/ISSN 1029-2470 online © 2006 Taylor & Francis
DOI: 10.1080/10715760500456219

and phototransduction [8]. Physiological amounts of NO synthesized by constitutive NOS isoforms (NOS-1 and NOS-3) participates in neurotransmission and vascular signaling [9] while accelerated NO production by NOS-2 results in cytotoxicity via direct reactions of NO and the formation of secondary species capable of oxidation and nitration reactions [10]. The oxidation and nitration of lipids, amino acids, and proteins will alter biomolecular structure and function and at the same time reveal the pathogenic actions of reactive species in various disease processes [11].

Altered production of NO in inflammatory diseases like uveitis or degenerative diseases like glaucoma suggests that it contributes to the pathological states. This study aimed to study retinal NOS-2 expression, retinal protein nitration and investigate retinal ganglion and glial cell death in experimental rat models of elevated IOP and uveitis. It is reported herein that increased retinal NOS-2 expression and excessive NO formation is accompanied by retinal protein nitration and apoptosis in elevated IOP and ocular inflammation.

Materials and methods

Animals

All experimental protocols conducted on rats were performed in accordance with the standards established by the Institutional Animal Care and Use Committee at Akdeniz University Medical School. Male Wistar rats weighing 350–450 g were housed in stainless steel cages and given food and water *ad libitum*. Animals were maintained at 12 h light–dark cycles and a constant temperature of 23 ± 1°C at all times. Rats were divided into four groups of six animals each; Group 1: elevated IOP, Group 2: LPS-treated, Group 3: elevated IOP + LPS-treated, Group 4: control.

Rat model of ocular inflammation and elevated IOP

Ocular inflammation was induced via a single injection of intra-vitreal LPS as previously described [12]. Briefly, LPS from Salmonella typhimurium (Sigma-Aldrich Chemie, Steinheim, Germany) was dissolved in sterile phosphate buffered saline (PBS) at a concentration of 1 mg/ml. Rats were anesthetized intraperitoneally with a mixture of ketamine (25 mg/kg, Richter Pharma AG, Wels, Austria) and xylazine hydrochloride (5 mg/kg, Alfasan International B.V., Woerden, Holland) and 5 μg of LPS was injected into the vitreous of each eye. The controls received intravitreal injections of LPS free PBS. Rats were killed 24 h after LPS injection and eyes were enucleated for further analysis.

IOP was elevated in rats by cauterizing three episcleral vessels, as previously [13,14] described. Briefly, rats were anesthetized intraperitoneally with a mixture of ketamine (25 mg/kg) and xylazine hydrochloride (5 mg/kg). Episcleral vessels were exposed by incising the overlying conjunctiva and cauterized via an ophthalmic cautery. IOP was measured before surgery and every 2 weeks after surgery over a 2-month period. A handheld tonometer (XL-Tonopen, Mentor O and O, Norwell, MA, USA) was used to measure IOP in rats under light anesthesia. One drop of 0.5% proparacaine hydrochloride was applied to each eye before readings were obtained. Intraocular pressure measurements were performed as described in the instruction manual of the tonometer. The mean IOP of 5–10 consecutive measurements were recorded. Rats in Group 3 (elevated IOP + LPS-treated) received a single injection of intra-vitreal LPS on the 60th day following episcleral cauterization.

Immunohistochemical staining and TUNEL analysis

Enucleated globe materials were fixed in 10% buffered formalin solutions and incised in transverse plain just from the center of the globe to obtain two equal parts. Fixed tissues were washed in phosphate buffered saline (pH 7.4), embedded in paraffin and cut into 4 μm sections. For peroxidase staining, sections were deparaffined, rehydrated and washed with Tris buffered saline. Endogenous peroxidase activity was blocked by incubating tissue sections with 3% hydrogen peroxide for 5 min prior to application of the primary antibody. Primary antibody incubations were for 60 min at 25°C using rabbit polyclonal anti-NOS2 (1:100 dilution, Santa Cruz Biotechnology, Santa Cruz, CA) and anti-nitrotyrosine (NO_2Tyr) (Cayman Chemical, Ann Arbor MI, 10 μg/ml). After sections were washed they were immunostained with an avidinbiotin complex kit (Dako, Carpinteria, CA) followed by hematoxylin counterstaining. To assess nonspecific staining for anti-NO_2Tyr, control experiments were performed by preadsorbing anti-NO_2Tyr with 10 mM NO_2Tyr. Negative controls were also performed by replacing the primary antibody with nonimmune serum followed by immunoperoxidase staining. Presence of a redbrown colored end product in the cytoplasm was indicative of positive staining. Counterstaining with hematoxylin resulted in a pale to dark blue coloration of cell nuclei.

Apoptotic cells were visualized with the terminal deoxynucleotide transferase (TdT) FragEL DNA fragmentation kit (Oncogene, Boston, MA) analogous to TdT mediated nick endlabeling. Dark brown cells with pyknotic nuclei were indicative of positive staining for apoptosis, whereas green to greenish color signified a nonreactive cell. To obtain a quantitative standard for apoptotic cell death within the different experimental group's morphometric

analysis was performed on all retinal sections by a pathologist blinded to the experimental conditions.

SDS-PAGE and Western blot analysis

Retina was harvested from enucleated globes and homogenized in 2 ml ice-cold homogenizing buffer (50 mM K_2HPO_4, 80 μM leupeptin, 2.1 mM Pefabloc SC, 1 mM phenylmethylsulfonyl fluoride, 1 μg/ml aprotinin, pH 7.4). Homogenates were centrifuged (40,000 *g*, 30 min, 4°C) and supernatants were stored at −80°C until analyzed. For western blot analysis, tissue proteins were separated by SDS-PAGE and transferred to nitrocellulose membranes. A rabbit polyclonal antibody against anti-NO_2Tyr (Cayman Chemical, 5 μg/ml) and anti-NOS2 (BD Transduction Laboratories, 1:800 dilution) was used for immunoblot analysis. Horseradish peroxidase-conjugated goat anti-rabbit IgG (Zymed Laboratories, San Francisco, CA, 1:10000 dilution) was used as a secondary antibody and immunoreactive proteins were visualized by chemiluminescence via ECL reagent (Amersham Pharmacia Biotech). Proteins separated by SDS-PAGE were also visualized by Electro-Blue staining solution (Qbiogene, Heidelberg, Germany).

Nitrite and nitrate assay

Samples were transferred to an ultrafiltration unit and centrifuged through a 10 kDa molecular mass cut-off filter (Centricon, Millipore Corporation) for 1 h to remove protein. Analyses of tissue homogenates were performed in duplicate via the Greiss reaction using a colorometric assay kit (Calbiochem, Darmstadt, Germany). Protein concentrations were measured at 595 nm by a modified Bradford assay by using Coomassie Plus reagent with bovine serum albumin as a standard (Pierce Chemical Company, Rockford, IL).

Results

IOP levels

The IOP (mean ± SD, $n = 6$) measured in control eyes were 10 ± 2.3 mm Hg. An increase of 10–12 mm Hg was observed in cauterized eyes compared to controls. Recorded IOP from cauterized eyes remained elevated over the 2 months experimental period.

Histologic analysis

Figure 1 shows photomicrographs of retinal cross sections from representative rats of each of the four different groups. Apparent differences were observed in the histologic evaluation of the retina. Groups treated with LPS (Figure 1(B) and (D)) displayed extensive polymorphonuclear (PMN) cell infiltration accompanied by retinal edema while retinal thinning was prominent in rats with elevated IOP (Figure 1(C)).

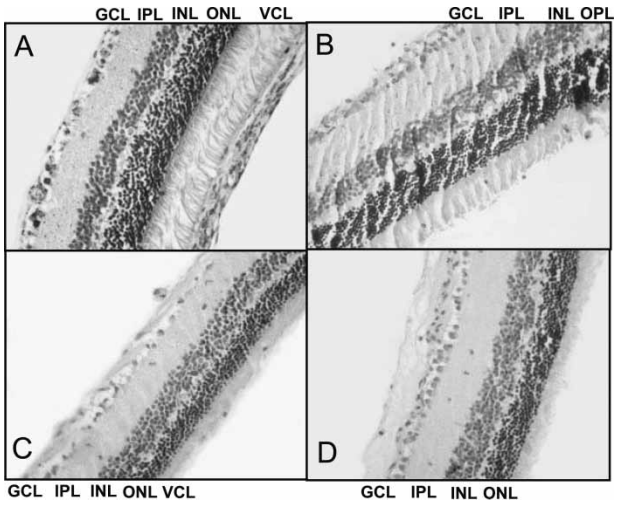

Figure 1. Hematoxylin and eosin staining of the retina. Retinal photomicrographs of representative rat are shown from each of the four groups. (A) Control, (B) LPS, (C) Elevated IOP, (D) Elevated IOP + LPS. GCL, ganglion cell layer; IPL, inner plexiform layer; INL, inner nuclear layer; ONL, outer nuclear layer; VCL, photoreceptor cell layer.

NOS-2 expression

Figure 2 demonstrates the localization of NOS-2 in retinal cross sections from representative rats of each

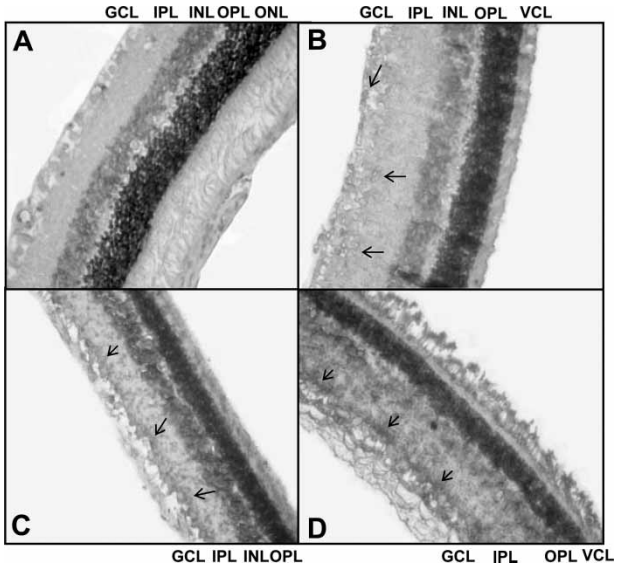

Figure 2. Immunostaining of NOS-2 in the Retina. Retinal photomicrographs (× 20) of representative rat are shown from each of the four groups. (A) Control, (B) LPS, (C) Elevated IOP, (D) Elevated IOP + LPS. GCL, ganglion cell layer; IPL, inner plexiform layer; INL, inner nuclear layer; ONL, outer nuclear layer; VCL, photoreceptor cell layer. Arrows show regions of NOS-2 immunostaining.

of the four different groups. NOS-2 positive staining was observed throughout the outer plexiform layer (OPL), inner plexiform layer (IPL) and ganglion cell layer (GCL) in all experimental groups except for control. The photoreceptor cell layer (VCL) also showed diffuse NOS-2 immunostaining in all diseased rats. NOS-2 was not present in eyes of control rats (Figure 2(A)). The quantitative data obtained for NOS-2 expression is shown in Figure 3. Western blot analysis of retinal extracts using an anti-NOS2 antibody revealed an immunodetectable 130 kDa protein band present only in diseased rat groups (Figure 3(A)). Elevated IOP and LPS treatment caused a significant increase in NOS-2 protein expression, as quantified by densitometric analysis, Figure 3(C) ($p < 0.05$, *vs* control). NOS-2 expression was further increased in rats with elevated IOP + LPS ($p < 0.05$, *vs* elevated IOP and LPS groups).

Nitrite and nitrate concentration

Vitreous and retinal tissue homogenate nitrite (NO_2^-) and nitrate (NO_3^-) concentration is shown in Figure 4. Vitreous $NO_2^- + NO_3^-$ levels (mean ± SEM, $n = 5-6$) measured in elevated IOP (158.5 ± 5.3 μM), LPS (243 ± 6.4 μM), and elevated IOP + LPS (415.3 ± 10.6 μM) groups were significantly greater ($p < 0.05$) than the control group (98 ± 7.1 μM). $NO_2^- + NO_3^-$ levels in the retina affirmed significantly increased levels of nitric oxide generation in LPS-treated rats with elevated IOP (346 ± 23.8 μM) *vs* LPS-treated, elevated IOP and control groups (195.6 ± 12.6, 130 ± 2.5 and 76.6 ± 15.6 μM, respectively). Elevated IOP + LPS further increased ($p < 0.05$) vitreous and retina $NO_2^- + NO_3^-$ levels when compared to rats with only elevated IOP or LPS.

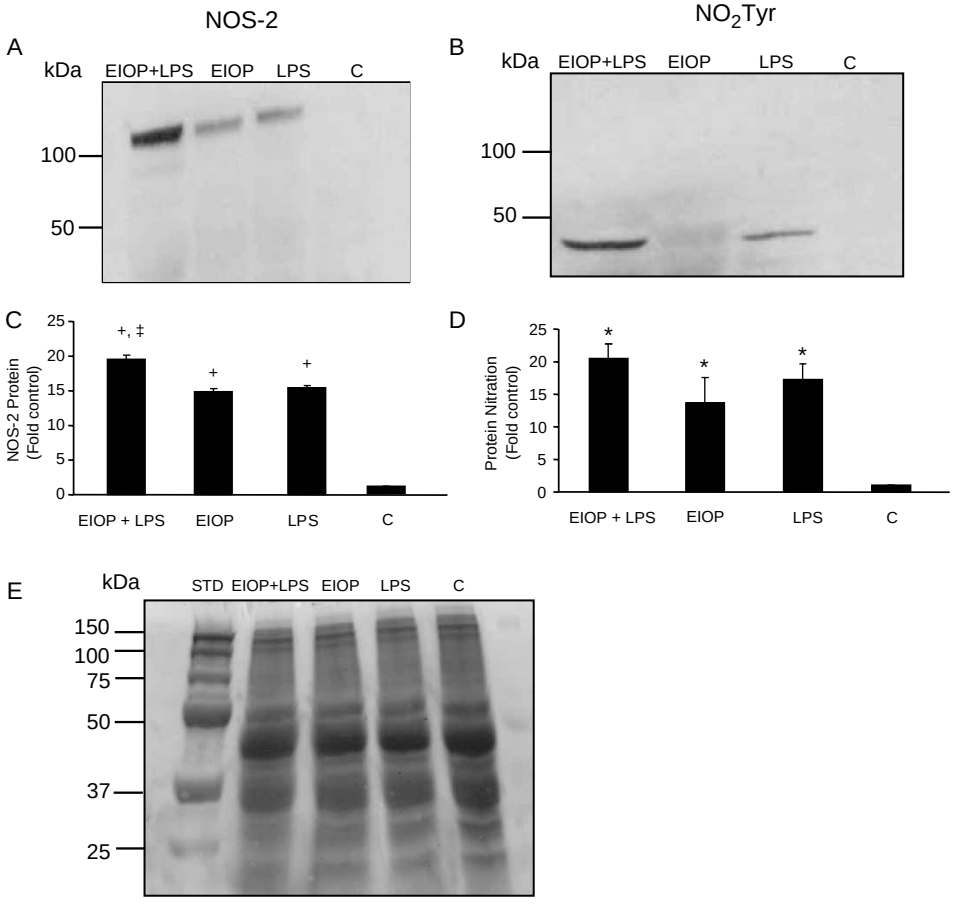

Figure 3. SDS-PAGE and Western blot analysis of retinal homogenates. STD, molecular weight standards; C, control; EIOP, elevated intraocular pressure; LPS, lipopolysaccharide-treated. Retinal homogenates analyzed by immunoblotting with rabbit polyclonal antibody against (A) NOS-2 and (B) nitrotyrosine. (C) and (D) represent averaged data quantified by densitometry of immunoblots using NIH image 1.61. Data are expressed as-fold increase, in which the control is defined as 1.0. Values are mean ± SEM for three independent experiments. Statistical analysis was by one-way ANOVA with all pairwise multiple comparison procedures carried out via Tukey Test. +, $p < 0.05$ compared to control; ‡, $p < 0.05$ compared to EIOP and LPS; ⋆, $p < 0.05$ compared to control. (E) SDS-PAGE and Coomassie blue staining of retinal homogenates.

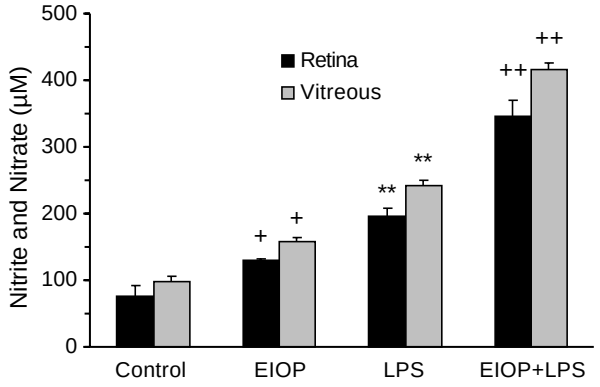

Figure 4. Vitreous and retinal tissue homogenate nitrite and nitrate content. C, control; EIOP, elevated intraocular pressure; LPS, lipopolysaccharide-treated. Values are mean ± SEM ($n = 5$–6). Statistical analysis was by Kruskal–Wallis one way analysis of variance on ranks with all pairwise multiple comparison procedures carried out via Dunn's Method. +, $p < 0.05$ compared to control; **, $p < 0.05$ compared to EIOP and control; ++, $p < 0.05$ compared to LPS, EIOP, and control.

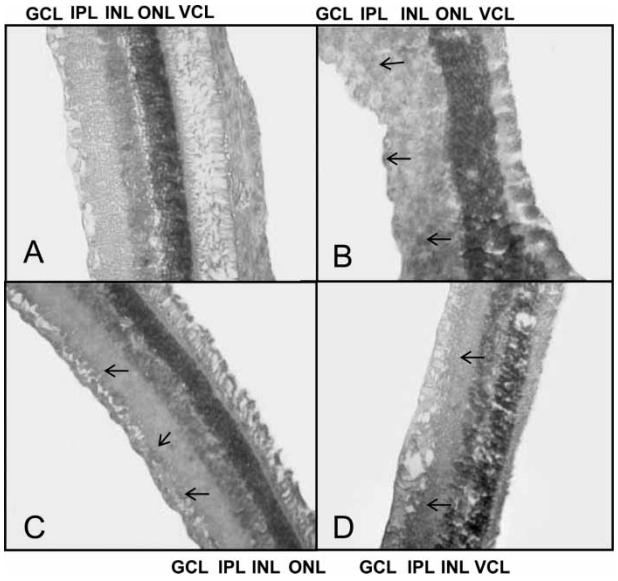

Figure 5. Immunostaining of nitrotyrosine in the Retina. Retinal photomicrographs (× 20) of representative rat are shown from each of the four groups. (A) Control, (B) LPS, (C) Elevated IOP, (D) Elevated IOP + LPS. GCL, ganglion cell layer; IPL, inner plexiform layer; INL, inner nuclear layer; ONL, outer nuclear layer; VCL, photoreceptor cell layer. Arrows show regions of NO_2-Tyr immunostaining.

Nitrotyrosine Formation

Samples from all experimental groups were analyzed by SDS-PAGE and visualized by both Western blot analysis using anti-NO_2Tyr antibody and Coomassie blue staining for proteins. Western blot analysis of retinal extracts using an anti-NO_2Tyr antibody revealed a single immunoreactive protein band with a molecular weight of less than 50 kDa. Comparison of the immunoreactivity pattern seen in the Western blots (Figure 3(B)) with protein staining (Figure 3(E)) reveals that retinal proteins are not equally nitrated. The quantitative data obtained for NO_2Tyr formation is shown in Figure 3(D) and represents averaged data quantified by densitometry of immunoblots. Protein nitration was present only in diseased rat groups and was more evident in elevated IOP + LPS treated rats. The localization of protein NO_2Tyr in retinal cross sections is demonstrated in Figure 5. NO_2Tyr positive staining was observed in the GCL, IPL and VCL in all rat groups except for controls.

Apoptosis

Figure 6 shows representative photomicrographs of retinal TUNEL staining from each of the four groups. Apoptotic cells are seen in the GCL, outer and inner nuclear layers of all diseased groups. Percent of TUNEL positive cells were significantly greater ($p < 0.05$) in both the ONL and INL of all diseased rat groups, compared to control (Figure 7). The greatest increase in the percent of apoptotic cells were observed in rats treated with elevated IOP + LPS.

Discussion

This study examined the effect of elevated IOP and ocular inflammation on retinal NOS-2 expression, protein nitration and apoptosis in experimental rat models. To accomplish intraocular pressure elevation, episcleral vessels of the eye were cauterized as previously described [13]. A 1.4-fold increase in IOP was observed in operated eyes following surgery, and persisted over the 2-month experimental period. The measured increase in IOP compared well to previous levels reported in rats [15,16]. The rat model of intraocular inflammation was created by intravitreal injection of LPS as previously described [12]. Reported studies have documented that this method of endotoxin-induced uveitis causes severe fibrinoid exudation in the papillary area with intense flare in the anterior chamber at 24 h after injection [17]. These symptoms compare to grade 4 (full score) uveitis [18] and thus enucleation was performed 24 h after LPS injection. In accordance with previous observations [12], histological examinations showed the presence of inflammatory cells in the inner retinal layers of LPS treated rats (Figure 1(B) and (D)).

The observed increase in NOS-2 protein in experimental rat models of elevated IOP and/or ocular inflammation (Figures 2 and 3) is consistent with the involvement of NO cytotoxicity in elevated IOP [7] and uveitis [12]. Reported studies have demonstrated the presence of NOS-2 mRNA in the iris-ciliary body and in the retina of rats with endotoxin-induced ocular

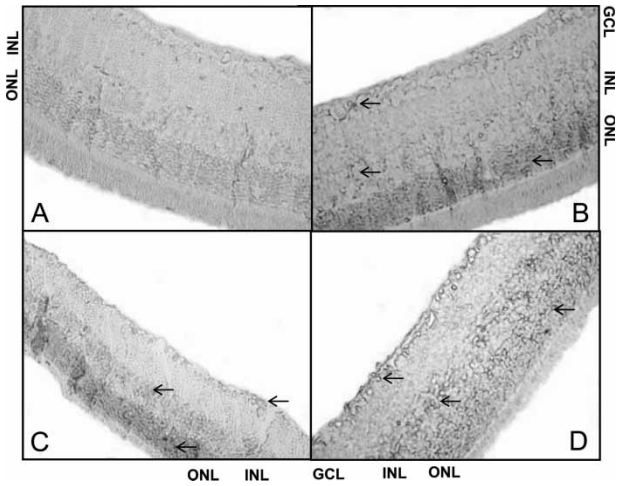

Figure 6. Retinal TUNEL staining. Photomicrographs (× 20) of representative rat are shown from each of the four groups. (A) Control, (B) LPS, (C) Elevated IOP, (D) Elevated IOP + LPS. Apoptotic cells are seen in the ganglion cell layer (GCL), outer (ONL) and inner (INL) nuclear layers of all diseased groups.

inflammation [19]. Moreover, a significant correlation was found between nitrite levels detected in the vitreous and clinical signs of endotoxin-induced uveitis [5]. Similarly, NOS-2 immunostaining was observed in glaucomatous optic nerve heads suggesting that it may contribute to retinal ganglion cell death associated with elevated IOP [7,20]. Indeed, pharmacological studies have shown that inhibition of NOS-2 by aminoguanidine provides neuroprotection of retinal ganglion cells in a rat model of chronic glaucoma [21]. Likewise, multiple intraperitoneal injections of L-NAME, a well-known NOS inhibitor, reduced clinical signs of uveitis in LPS-injected rats [22], suggesting that NO could participate to the pathogenesis of endotoxin-induced uveitis as a proinflammatory mediator. NOS-2 positive staining observed throughout the OPL, IPL and GCL (Figure 2) is also supportive of previous studies which have identified retinal NOS-2 production in pigmented epithelial cells [23], vascular endothelium [24] and Müller cells [6], that span the entire thickness of the retina.

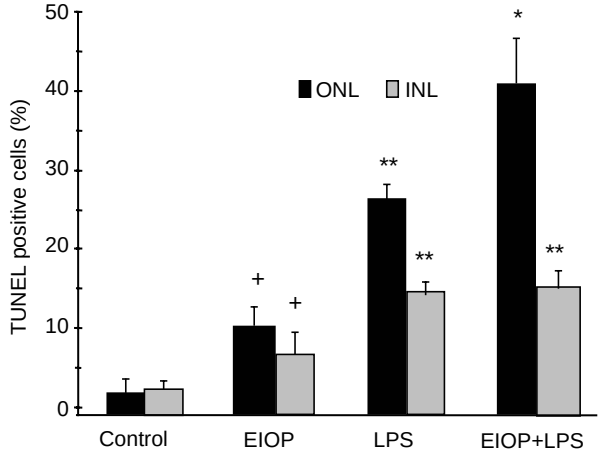

Figure 7. Percent of apoptotic cells in the outer (ONL) and inner nuclear layers (INL) of the retina. C, control; EIOP, elevated intraocular pressure; LPS, lipopolysaccharide-treated. Values are mean ± SD ($n = 6$). Statistical analysis was by one-way ANOVA with all pairwise multiple comparison procedures carried out via Tukey Test. +, $p < 0.05$ *vs* control; **, $p < 0.05$ *vs* EIOP and control; *, $p < 0.05$ *vs* LPS, EIOP and control.

Nitration of tyrosine residues has been detected in multiple species, organ systems, and cell types during both acute and chronic inflammation [25]. The existence of multiple distinct, yet redundant pathways for tyrosine nitration underscores the potential significance of this process in inflammation and cell signaling. This post-translational protein modification is thus a marker of oxidative injury that is frequently linked to altered protein function during inflammatory conditions [25,26]. Previous reports have revealed the occurrence of oxidative stress in glaucomatous optic nerve damage [27,28] and ocular inflammation [29]. Elevated expression of NOS-2 in both of these diseases implies the formation of secondary species capable of nitration reactions. Indeed, nitration of protein-associated tyrosine residues has been detected in rats groups with elevated IOP, LPS and elevated IOP + LPS (Figures 2 and 3). The significant increase of NO_2Tyr observed in rats with elevated IOP + LPS (Figure 3(B) and (D)) suggests that elevated IOP and ocular inflammation is additive in contributing to oxidative stress and NOS-2 expression resulting in the formation of nitration reactions.

Nitric oxide-mediated cytotoxicity and the capacity of NO to induce apoptosis have been documented in macrophages [30], astrocytes [31], and neuronal cells [32]. Although the mechanisms of NO-mediated apoptosis are not clearly elucidated, the induction of apoptosis by NO can be the result of DNA damage which in turn activates p53 that has been reported to cause apoptosis [33]. Increased apoptotic cells in the GCL, outer and inner nuclear layers of the retina in all diseased groups (Figures 6 and 7) is supportive of NOS-2 induced apoptosis and suggests that elevated IOP and LPS may aggravate pathogenic changes in the retina by stimulating NO production.

In summary, the present data illustrates that both elevated IOP and ocular inflammation augment NOS-2 expression, retinal protein nitration and apoptosis in rats. Although results show increased IOP and LPS have additive effects on nitration and apoptosis, it is uncertain if these findings are related. Obtained data suggests that protein nitration and apoptosis exacerbate disease progression in clinical conditions accompanied by elevated IOP and ocular inflammation. Thus, selective inhibiton of NOS-2 and appropriate IOP-lowering may prevent long-term

visual loss and lead to improvement in the management of glaucoma secondary to uveitis.

Acknowledgements

We are grateful to Dr Bruce A. Freeman for his valuable contribution. This study was supported by a grant from Akdeniz University Research Foundation, Antalya, Turkey (2003.01.0103.007)

References

[1] Lee DA, Higginbotham EJ. Glaucoma and its treatment: A review. Am J Health Syst Pharm 2005;62:691–699.

[2] Gaasterland D, Tanishima T, Kuwabara T. Axoplasmic flow during chronic experimental glaucoma. I. Light and electron microscopic studies of the monkey optic nervehead during development of glaucomatous cupping. Invest Ophthalmol Vis Sci 1978;17:838–846.

[3] Quigley HA, Addicks EM. Chronic experimental glaucoma in primates. II. Effect of extended intraocular pressure elevation on optic nerve head and axonal transport. Invest Ophthalmol Vis Sci 1980;19:137–152.

[4] Rothova A, Suttorp-van Schulten MS, Frits Treffers W, Kijlstra A. Causes and frequency of blindness in patients with intraocular inflammatory disease. Br J Ophthalmol 1996;80:332–336.

[5] Mandai M, Yoshimura N, Yoshida M, Iwaki M, Honda Y. The role of nitric oxide synthase in endotoxin-induced uveitis: Effects of NG-nitro L-arginine. Invest Ophthalmol Vis Sci 1994;35:3673–3680.

[6] Goureau O, Hicks D, Courtois Y, De Kozak Y. Induction and regulation of nitric oxide synthase in retinal Muller glial cells. J Neurochem 1994;63:310–317.

[7] Shareef S, Sawada A, Neufeld AH. Isoforms of nitric oxide synthase in the optic nerves of rat eyes with chronic moderately elevated intraocular pressure. Invest Ophthalmol Vis Sci 1999;40:2884–2891.

[8] Becquet F, Courtois Y, Goureau O. Nitric oxide in the eye: Multifaceted roles and diverse outcomes. Surv Ophthalmol 1997;42:71–82.

[9] Goldstein IM, Ostwald P, Roth S. Nitric oxide: A review of its role in retinal function and disease. Vision Res 1996;36:2979–2994.

[10] Schopfer FJ, Baker PR, Freeman BA. NO-dependent protein nitration: A cell signaling event or an oxidative inflammatory response? Trends Biochem Sci 2003;28:646–654.

[11] Ischiropoulos H. Biological tyrosine nitration: A pathophysiological function of nitric oxide and reactive oxygen species. Arch Biochem Biophys 1998;356:1–11.

[12] Koga T, Koshiyama Y, Gotoh T, Yonemura N, Hirata A, Tanihara H, Negi A, Mori M. Coinduction of nitric oxide synthase and arginine metabolic enzymes in endotoxin-induced uveitis rats. Exp Eye Res 2002;75:659–667.

[13] Sawada A, Neufeld AH. Confirmation of the rat model of chronic, moderately elevated intraocular pressure. Exp Eye Res 1999;69:525–531.

[14] Yucel I, Akar Y, Yucel G, Ciftcioglu MA, Keles N, Aslan M. Effect of hypercholesterolemia on inducible nitric oxide synthase expression in a rat model of elevated intraocular pressure. Vision Res 2005;45:1107–1114.

[15] Shareef SR, Garcia-Valenzuela E, Salierno A, Walsh J, Sharma SC. Chronic ocular hypertension following episcleral venous occlusion in rats. Exp Eye Res 1995;61:379–382.

[16] Cabrera CL, Wagner LA, Schork MA, Bohr DF, Cohan BE. Intraocular pressure measurement in the conscious rat. Acta Ophthalmol Scand 1999;77:33–36.

[17] Rosenbaum JT, McDevitt HO, Guss RB, Egbert PR. Endotoxin-induced uveitis in rats as a model for human disease. Nature 1980;286:611–613.

[18] Ruiz-Moreno JM, Thillaye B, de Kozak Y. Retino-choroidal changes in endotoxininduced uveitis in the rat. Ophthalmic Res 1992;24:162–168.

[19] Goureau O, Bellot J, Thillaye B, Courtois Y, de Kozak Y. Increased nitric oxide production in endotoxin-induced uveitis. Reduction of uveitis by an inhibitor of nitric oxide synthase. J Immunol 1995;154:6518–6523.

[20] Liu B, Neufeld AH. Expression of nitric oxide synthase-2 (NOS-2) in reactive astrocytes of the human glaucomatous optic nerve head. Glia 2000;30:178–186.

[21] Neufeld AH, Sawada A, Becker B. Inhibition of nitric-oxide synthase 2 by aminoguanidine provides neuroprotection of retinal ganglion cells in a rat model of chronic glaucoma. Proc Natl Acad Sci USA 1999;96:9944–9948.

[22] Parks DJ, Cheung MK, Chan CC, Roberge FG. The role of nitric oxide in uveitis. Arch Ophthalmol 1994;112:544–546.

[23] Goureau O, Lepoivre M, Becquet F, Courtois Y. Differential regulation of inducible nitric oxide synthase by fibroblast growth factors and transforming growth factor beta in bovine retinal pigmented epithelial cells: Inverse correlation with cellular proliferation. Proc Natl Acad Sci USA 1993;90:4276–4280.

[24] Chakravarthy U, Stitt AW, McNally J, Bailie JR, Hoey EM, Duprex P. Nitric oxide synthase activity and expression in retinal capillary endothelial cells and pericytes. Curr Eye Res 1995;14:285–294.

[25] Ischiropoulos H, Gow A. Pathophysiological functions of nitric oxide-mediated protein modifications. Toxicology 2005;208:299–303.

[26] Aslan M, Ryan TM, Townes TM, Coward L, Kirk MC, Barnes S, Alexander CB, Rosenfeld SS, Freeman BA. Nitric oxide-dependent generation of reactive species in sickle cell disease. Actin tyrosine induces defective cytoskeletal polymerization. J Biol Chem 2003;278:4194–4204.

[27] Ferreira SM, Lerner SF, Brunzini R, Evelson PA, Llesuy SF. Oxidative stress markers in aqueous humor of glaucoma patients. Am J Ophthalmol 2004;137:62–69.

[28] Izzotti A, Sacca SC, Cartiglia C, De Flora S. Oxidative deoxyribonucleic acid damage in the eyes of glaucoma patients. Am J Med 2003;114:638–646.

[29] Satici A, Guzey M, Gurler B, Vural H, Gurkan T. Malondialdehyde and antioxidant enzyme levels in the aqueous humor of rabbits in endotoxin-induced uveitis. Eur J Ophthalmol 2003;13:779–783.

[30] Sarih M, Souvannavong V, Adam A. Nitric oxide synthase induces macrophage death by apoptosis. Biochem Biophys Res Commun 1993;191:503–508.

[31] Hu J, Van Eldik LJ. S100 beta induces apoptotic cell death in cultured astrocytes via a nitric oxide-dependent pathway. Biochim Biophys Acta 1996;1313:239–245.

[32] Heneka MT, Loschmann PA, Gleichmann M, Weller M, Schulz JB, Wullner U, Klockgether T. Induction of nitric oxide synthase and nitric oxide-mediated apoptosis in neuronal PC12 cells after stimulation with tumor necrosis factor-alpha/lipopolysaccharide. J Neurochem 1998;71:88–94.

[33] Kim YM, Bombeck CA, Billiar TR. Nitric oxide as a bifunctional regulator of apoptosis. Circ Res 1999;84:253–256.